

A Simple Class Decision Balancing for Incremental Learning

Hongjoon Ahn¹ and Taesup Moon^{1,2}

¹ Department of Artificial Intelligence

² Department of Electrical and Computer Engineering
Sungkyunkwan University, Suwon, Korea 16419
{hong0805, tsmoon}@skku.edu

Abstract. Class incremental learning (CIL) problem, in which a learning agent continuously learns new classes from incrementally arriving training data batches, has gained much attention recently in AI and computer vision community due to both fundamental and practical perspectives of the problem. For mitigating the main difficulty of deep neural network(DNN)-based CIL, the catastrophic forgetting, recent work showed that a simple fine-tuning (FT) based schemes can outperform the earlier attempts of using knowledge distillation, particularly when a small-sized exemplar-memory for storing samples from the previously learned classes is allowed. The core limitation of the vanilla FT, however, is the severe classification score bias between the new and previously learned classes, and several state-of-the-art methods proposed to rectify the bias via additional post-processing of the scores. In this paper, we propose two simple modifications for the vanilla FT, *separated softmax* (SS) layer and *ratio-preserving* (RP) mini-batches for SGD updates. Our scheme, dubbed as SS-IL, is shown to give much more balanced class decisions, have much less biased scores, and outperform strong state-of-the-art baselines on several large-scale benchmark datasets, *without any* sophisticated post-processing of the scores. We also give several novel analyses our and baseline methods, confirming the effectiveness of our approach in CIL.

Keywords: Class incremental learning, catastrophic forgetting, fine-tuning, exemplar-memory

1 Introduction

Incremental or continual learning, in which the agent continues to learn with incremental arrival of new training data, is one of the grand challenges in artificial intelligence and machine learning. Such setting, which does not assume the full availability of the old training data, is recently gaining more attention particularly from the real-world application perspective. The reason is because storing all the training data, which can easily become large-scale, in one batch often becomes unrealistic for memory- and computation-constrained applications, such as mobile phones or robots, hence the continuous yet effective update of the learning agent without accessing the full data received so far is indispensable.

A viable candidate for such agent is the end-to-end learning based deep neural network (DNN) models. Following the recent success of DNN in many different applications [14,3,5], the DNN-based incremental learning methods have been also actively

pursued in recent years. Although they achieved some promising results, they also possess a critical limitation: the *catastrophic forgetting*, which refers to the problem that the generalization performance on the old data severely degrades after a naive fine-tuning of the model with the new data.

In this paper, we focus on the DNN-based *class* incremental learning (CIL) problem, which we refer to learning a classifier to classify *new* object classes from every incremental training data and testing the classifier on all the classes learned so far. Among several different proposed approaches, the exemplar-memory based approach [26,4], which allows to store small amount of training data from old classes in a separate memory, has attained promising results. It has been shown that using the small exemplar memory plays an important role in mitigating the catastrophic forgetting, and allowing such small size of memory while learning is also tolerable in practical scenarios as well.

The main challenge of using the exemplar-memory is to resolve the severe data imbalance issue between the training data points for the new classes and those for the old classes in the exemplar-memory. That is, the naive fine-tuning (FT) with such imbalanced data may still heavily skew the predictions toward the newly learned classes, hence, the accuracy for the old classes would dramatically drop, still resulting in significant forgetting. To that end, several attempts have been made to resolve such data imbalance problem of the exemplar-memory based CIL algorithms. Knowledge distillation [15] based methods [26,6] were the initially proposed methods, while more recent state-of-the-arts include explicit steps for post-processing of the classification scores of the vanilla FT-based methods, that are biased toward the new classes [4,28]. The common reasoning of the latter schemes were from the finding that the classification scores for the newly learned classes after fine-tuning tend to have much higher values than those of the old classes [4, Figure2], thus, explicitly correcting that bias *after* learning the model could improve the accuracy on all classifying classes.

Our proposing method is based on the similar motivation as [4,28] that the heavy classification score bias toward new classes exists. However, instead of devising a separate bias correction step, we make two *simple but subtle* modifications of the vanilla fine-tuning (FT) method such that the learned model can naturally make the balanced predictions among old and new classes without any score post-processing steps. The modifications follow from the observation that the gradient of the classification score (in the softmax output layer) for the non-target class is always positive. Therefore, when fine-tuning the model with the imbalanced data biased toward the new class data, the classification scores of the old classes would continue to drop during the gradient descent steps computed from the training samples for the new classes. We believe this simple observation, which has not been explicitly elaborated in previous work, explains the heavy score bias of the fine-tuned model.

From above observation, we propose Separated Softmax for IL (SS-IL) which makes the following two modifications for the vanilla fine-tuning (FT): (1) *separated softmax* (SS) layer that mutually blocks the flow of the score gradients between the old and new classes, and (2) *ratio-preserving* (RP) *mini-batch* that always maintains the relative ratio between the old and new class examples for the stochastic gradient descent (SGD). With these simple modifications, we show in our experiments that our SS-IL outperforms the recent state-of-the-art baselines, e.g., IL2M [4], without any additional post-processing

of the classification scores. We also show detailed ablation study on our method as well as analysis results on why the post-processing as in [4] can be unreliable.

2 Related Work

In this section, we summarize algorithms related to continual learning and class incremental learning (CIL). Here, the algorithms denoted by “continual learning” make an assumption that task information is available at the test time, and the algorithms denoted by “class incremental learning”, the focus of this paper, does not make such assumption. Hence, the CIL deals with a more challenging setting than the continual learning algorithms mentioned below.

Regularization based continual learning In regularization based approaches, they try to prevent catastrophic forgetting by measuring the importance of each model weight, and giving high regularization penalty on important weights to prevent weight change. A well known method, [19], defines the importance of weights as the diagonal elements of the Fisher information matrix, and a similar approach, [30], uses the path integral value as penalty strength. [7], which is a combination of [19] and [30], utilizes both Fisher information and path integral value. A slightly different approach, [24], tries to approximate the model distributions by measuring the uncertainty of each weight using variational inference, and prevent distribution shift using Bayesian online learning. In [2], which is a variant of [24], instead of measuring the uncertainty of each weight, they measure the uncertainty of each node and introduce an adaptive gracefully forgetting method.

Memory based continual learning In memory based approaches, they try to construct an exemplar by storing small subset of previous task data, and utilize the information in exemplar to prevent catastrophic forgetting. In [22], they solves the constrained optimization problem by using gradients for each task using exemplars. However, due to hard constraint on the gradient of each task, new tasks become harder to learn. To overcome this issue, the constraint relaxed version, [8], tries to compute the average of the gradient, and solves a much simpler constrained optimization problem. In [9], instead of computing gradients, they concatenate two batches which are drawn from exemplar and current task dataset.

Generative replay based continual learning and class incremental learning In generative replay based approaches, they generate the auxiliary data on previous tasks to prevent catastrophic forgetting. In [27], using Generative Adversarial Network(GAN)[11], they generate the previous task data and consider the “continual learning” scenario. In [18], they generate the features of old classes from a pre-trained model using stored class statistics, and apply it to the “class incremental learning” scenario. However, they have a limitation that they only generate the features on fully connected layer. To overcome this limitation, [29] tries to generate the intermediate feature of pre-trained network using Conditional GAN[23].

Knowledge distillation based class incremental learning and bias removal methods The earliest of knowledge distillation based methods, [21], uses knowledge distillation to keep the logit of previous tasks when learning new tasks. The developed version of [21], iCaRL [26], which uses memory exemplar, preserves the feature using knowledge distillation and then classifies the classes using the Nearest Mean of Exemplars (NME)

classification. However, the methods using exemplar, such as iCaRL, has been shown experimentally that there is a bias in the final FC layer. To tackle this problem, bias removal techniques [6,20,16,28] are proposed. In [6], to remove the prediction bias, they proposed a balanced fine-tuning method, which is fine-tuning the network using a balanced dataset. Another balanced fine-tuning approach [20], proposed a gradient scaling to remove the prediction bias. In [16], the cosine normalization is used to fix the norm of the weight of the linear classifier, which eliminates the bias, but still does not eliminate the problem of bias in the softmax probability. In [28], after the training, the bias correction layer was fine-tuned and removed using the validation set. Unlike the above methods, [4] proposed a post-processing approach, which rectify the output softmax probability using the statistics of the previous task prediction.

3 Notations and Problem Setting

In CIL, we assume every incrementally arrived training data, which is often called as the incremental *state*, consists of data for the *new* m classes that have not been learned before. More formally, the training data for the incremental state t is denoted by $\mathcal{D}_t = \{(\mathbf{x}_{ti}, y_{ti})\}_{i=1}^n$, in which \mathbf{x}_{ti} is the input data and $y_{ti} \in \{m(t-1) + 1, \dots, mt\}$ is the corresponding label. When learning each incremental state, we assume a separate exemplar-memory \mathcal{M} is allocated to store exemplar data for old classes. Namely, when learning the incremental state t , we store $\lfloor \frac{|\mathcal{M}|}{m(t-1)} \rfloor$ data points from each class that are learnt until the incremental state $t-1$. Thus, as the incremental state grows, the number of exemplar data points stored for each class decreases linearly with t . Also, we assume $|\mathcal{M}| \ll n$ and the total number of incremental states is denoted by T .

Our classification model consists of a feature extractor, which has the deep convolutional neural network (CNN) architecture, and the classification layer, which is the final fully-connected (FC) layer with softmax output. We denote $\boldsymbol{\theta}$ as the parameters for the feature extractor $\varphi(\cdot, \boldsymbol{\theta}) : \mathbf{x} \rightarrow \mathbb{R}^d$, which is shared throughout learning all incremental states, and $\mathbf{w}_t \in \mathbb{R}^{d \times m}$ as the parameter matrix for the FC layer associated with the incremental state t . Note the i -th column of the matrix, \mathbf{w}_{ti} , is used to compute the score of the class $m(t-1) + i$ ³.

At incremental state t , the parameters of the model, $\boldsymbol{\theta}$ and $\mathbf{W}_t \triangleq [\mathbf{w}_1, \dots, \mathbf{w}_t] \in \mathbb{R}^{d \times mt}$, are updated or learned using $\mathcal{D}_t \cup \mathcal{M}$. After learning, the prediction for a test sample \mathbf{x}_{test} is obtained by

$$\hat{y}_{\text{test}} = \arg \max_{y \in \{1, \dots, mt\}} \varphi(\mathbf{x}_{\text{test}}, \boldsymbol{\theta})^\top \mathbf{W}_{ty}, \quad (1)$$

in which \mathbf{W}_{ty} is the y -th column of \mathbf{W}_t . Namely, at test time, the final FC layers are consolidated and the prediction among all the classes in $\{1, \dots, mt\}$ is made as if running an ordinary multi-class classifier.

³ For notational brevity, we assume $\varphi(\mathbf{x}, \boldsymbol{\theta})$ also has a constant feature and \mathbf{w}_t includes the bias parameter.

4 Motivation

As mentioned in the Introduction, several previous work [6,20,16,28,4] identified that the major challenge of the exemplar-memory based CIL is resolving the classification score bias that a vanilla FT method suffers from. Here, we present the observation given in the Introduction more in details, and motivate our SS-IL.

Once the FT with the imbalanced $\mathcal{D}_t \cup \mathcal{M}$ is done, both the feature extractor $\varphi(\cdot, \theta)$ and the FC layer \mathbf{W}_t get updated. One may hypothesize that the severe score bias may be caused by the catastrophic forgetting phenomenon of θ and \mathbf{W}_t ; i.e., the feature extractor and the FC layer for the old classes have all significantly altered such that the model cannot classify the old classes well and think most of the test samples as the new class samples. We, however, argue that this is not the case and relative scale difference of the scores caused by the ordinary softmax training of FT would be the root cause of the score bias.

The top plot in Figure 1 shows the *average state-specific accuracy* on ILSVRC [10] of the vanilla FT based CIL and IL2M [4], in which we set $m = 100$, $T = 10$, and $|\mathcal{M}| = 10k$. Namely, after learning incremental state t , the prediction for each test example is done by only using the output FC layer specific to the state that the true class belongs to and the average accuracy of such prediction is reported. From the figure, we observe that the average state-specific accuracy does not catastrophically drop with the increased incremental state for both vanilla FT and IL2M. This genie-aided test result suggests that the feature extractor, the ResNet-18 [12] model in our experiment, as well as the state-specific FC layers in fact do *not* suffer from significant forgetting due to the imbalanced training data, thanks to the availability of the exemplar-memory.

We instead find the reason for the score bias in the well-known gradient form for the softmax classifier. That is, by denoting $s_j = \varphi(\mathbf{x}, \theta)^\top \mathbf{W}_{tj}$ as the classification score of input \mathbf{x} for class $j \in \{1 \dots, mt\}$, it is well-known that the gradient of the cross-entropy loss, \mathcal{L}_{CE} , with respect to s_j for the ordinary softmax output becomes

$$\frac{\partial \mathcal{L}_{\text{CE}}}{\partial s_j} = p_j - \mathbb{1}_{\{j=y\}}, \quad (2)$$

in which y is the ground-truth label for \mathbf{x} , $\mathbb{1}_{\{j=y\}}$ is the indicator for $j = y$, and $p_j = e^{s_j} / (\sum_{i=1}^{mt} e^{s_i})$. Since (2) is always positive for $j \neq y$, we can easily observe that when fine-tuning the model with $\mathcal{D}_t \cup \mathcal{M}$, the classification scores for the old classes will continue to peel off during the gradient descent steps done for the abundant samples for the new classes in \mathcal{D}_t . Thus, while the discriminative power of each state-specific

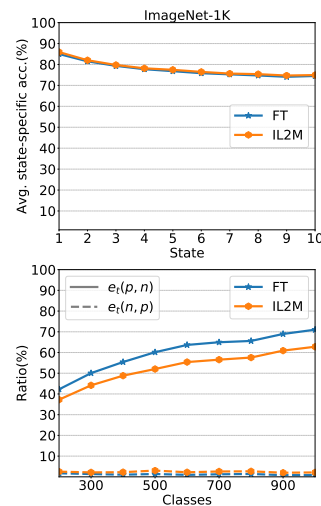


Fig. 1. Top: The average state-specific accuracy for each incremental state. Bottom: $e_t(p, n)$ and $e_t(n, p)$ for vanilla FT and IL2M. All the results are on ILSVRC dataset with $m = 100$ and $|\mathcal{M}| = 10k$

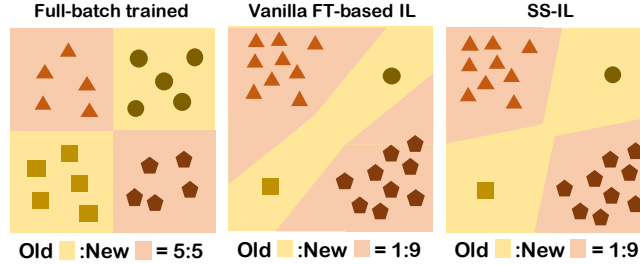


Fig. 2. Toy illustrations of decision boundaries for classifiers obtained by full balanced batch training (left), vanilla FT-based IL with exemplar-memory (center), and our SS-IL (right).

FC layer is not significantly hurt via incremental learning as shown in the top plot of Figure 1, we believe it is this imbalanced gradient descent steps for the classification scores for old classes that makes the significant score bias toward the new classes. IL2M [4], a current state-of-the-art CIL method, makes post-processing of the classification scores of vanilla FT based on the mean statistics of the scores in the training sets.

The bottom plot of Figure 1, however, shows that the bias correction of IL2M is not enough for sufficiently balancing the predictions between the old and new classes. The plot shows two error rates for each incremental state t , $e_t(p, n)$ and $e_t(n, p)$, which are defined to be the ratios of the old class test samples misclassified to the new classes and the new class test samples misclassified to the old classes, respectively, for both vanilla FT and IL2M. We observe that while IL2M corrects the skewness of the error rates of FT to some extent, it is still heavily biased; namely, $e_t(p, n)$ is much higher than $e_t(n, p)$, hence, majority of the old class samples are misclassified to the new classes, and such skewness gets worse as the incremental state increases. In Section 6.4, we also give in-depth analysis on the limitation of IL2M.

Our simple modifications of the vanilla FT based IL, which we elaborate in the next section, are motivated by above arguments and observations. Figure 2 shows toy illustration of the decision boundaries for the classifier obtained by full batch training, vanilla FT-based IL, and our SS-IL, respectively. Namely, our SS-IL aims to obtain a more balanced decision boundary, or the balanced score distribution, even with the heavily imbalanced training set, i.e., $\mathcal{D}_t \cup \mathcal{M}$.

5 Separated Softmax for Incremental Learning (SS-IL)

As outlined in the Introduction, our SS-IL consists of two simple modifications of vanilla FT, separated softmax (SS) layer and ratio-preserving (RP) mini-batch selection. Before concretely presenting them, we introduce some additional notations. For the incremental state t , we denote the class of old classes by $\mathcal{P}_t = \{1, \dots, m(t-1)\}$ and the class of new classes by $\mathcal{N}_t = \{m(t-1) + 1, \dots, mt\}$. Moreover, for a training data sample $(\mathbf{x}_i, y_i) \in \mathcal{D}_t \cup \mathcal{M}$, we denote $s_{ij} = \varphi(\mathbf{x}_i, \boldsymbol{\theta})^\top \mathbf{W}_{tj}$ as the classification score of \mathbf{x}_i for class $j \in \mathcal{P}_t \cup \mathcal{N}_t$

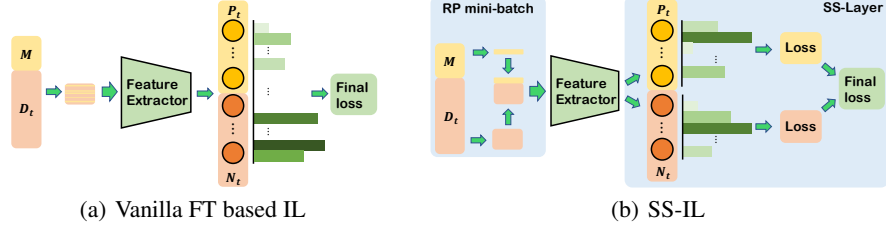


Fig. 3. Illustration of vanilla fine-tuning (FT) and our SS-IL.

Separated softmax (SS) layer: For $(\mathbf{x}_i, y_i) \in \mathcal{D}_t \cup \mathcal{M}$, we define a separate softmax output layer by defining the loss function as

$$\ell((\mathbf{x}_i, y_i), \boldsymbol{\theta}, \mathbf{W}_t) = -\log\left(\frac{e^{s_{y_i}}}{\sum_{j \in \mathcal{P}_t} e^{s_{ij}}}\right) \cdot \mathbb{1}\{y_i \in \mathcal{P}_t\} - \log\left(\frac{e^{s_{y_i}}}{\sum_{j \in \mathcal{N}_t} e^{s_{ij}}}\right) \cdot \mathbb{1}\{y_i \in \mathcal{N}_t\}. \quad (3)$$

Namely, depending on whether $(\mathbf{x}_i, y_i) \in \mathcal{M}$ or $(\mathbf{x}_i, y_i) \in \mathcal{D}_t$, we compute the separate softmax probability to compute the cross-entropy loss confined only for the classes in \mathcal{P}_t or \mathcal{N}_t , respectively. While (3) is a simple modification of the ordinary cross-entropy with softmax output on *all* classes, we can now see that $\frac{\partial \ell}{\partial s_{ij}} = 0$ for $j \in \mathcal{P}_t$ when $(\mathbf{x}_i, y_i) \in \mathcal{D}_t$. Therefore, fine-tuning with the new class samples will *not* have the overly penalizing effect in the classification scores for the old classes.

Ratio-preserving (RP) mini-batch: Another subtle change we implement for our SS-IL is the ratio-preserving (RP) mini-batches for the SGD updates of the model. Note when random mini-batches are sampled from $\mathcal{D}_t \cup \mathcal{M}$ for SGD, the severe imbalance between new and old classes carries over to the mini-batches as well. Such imbalance in mini-batches would significantly downplay the updates of the model for the old classes in our SS layer, since the gradient from the first part of (3) will be generated scarcely. From this observation and to assure the main role of exemplars in \mathcal{M} , *i.e.*, to fine-tune the representations and decision boundaries of old classes in response to learning the new classes in \mathcal{D}_t , we always generate the mini-batches such that the ratio between the samples from \mathcal{M} and \mathcal{D}_t is preserved. Motivated by Experience Replay [9] method, this can be simply implemented by concatenating the fixed size of random samples from \mathcal{M} , denoted by *replay batch* ($B_{\mathcal{M}}$) in the later sections, with the random samples from \mathcal{D}_t ($B_{\mathcal{D}_t}$). In our experiments, we set the ratio of new class samples over the old class samples to $2 \sim 8$ to set the balance between learning new classes and fine-tuning the knowledge learned for old classes.

Figure 3 illustrates difference between our SS-IL and the vanilla FT-based IL and Algorithm 1 summarizes our method. We show in our experimental results that our simple modification of vanilla FT can lead to more balanced class predictions as well as higher accuracy in CIL without *any* sophisticated post-processings of the classification scores.

6 Experiments

In this section, we compared our SS-IL with other state-of-the-art CIL methods with various experimental scenarios. For evaluation, we used two large scale datasets: ILSVRC 2012 (ImageNet) [10] and Google Landmark Dataset v2 (Landmark-v2) [1]. In addition, extensive analyses are carried out to show the effectiveness of SS-IL, and the importance of each component of the proposed method is analyzed through ablation study.

6.1 Datasets and evaluation protocol

For ImageNet and Landmark-v2 datasets, we use all classes in ImageNet dataset, and choose 1,000 and 10,000 classes in Landmark-v2 dataset to make two variations. The detailed explanation on each dataset is as follows:

ImageNet: ILSVRC 2012 dataset consists of 1,000 classes, which has nearly 1,300 images per class. By following the benchmark protocol in [26], we arranged the classes in a fixed random order. We experimented with varied total number of incremental states, $T = \{5, 10, 20\}$, which corresponds to $m = \{200, 100, 50\}$ per state, and for the exemplar-memory size, we used $|\mathcal{M}| = \{5000, 10000, 20000\}$. When constructing exemplar-memory, we used Ringbuffer approach proposed in [9], which simply random samples from old classes. Furthermore, as shown in Section 3, we always maintain balanced number of exemplars across all the old classes. Thus, as the incremental state increases, we delete equal number of exemplars from the old classes and add exemplars for the newly learned classes. For the evaluation of CIL models, we used ILSVRC 2012 validation set for testing.

Landmark-v2: Google Landmark Dataset v2 consists of 203,094 classes, and each class has $1 \sim 10247$ images. Since the dataset is highly imbalanced, we sampled 1,000 and 10,000 classes in the order of largest number of samples per class. We denote Landmark-v2 dataset with 1,000 and 10,000 classes as Landmark-v2-1K and Landmark-v2-10K, respectively. After sampling the classes, we arranged the classes in a fixed random order. Similarly as in ImageNet, we varied the total number of incremental states as $T = \{5, 10, 20\}$, which corresponds to $m = \{200, 100, 50\}$ in Landmark-v2-1K and $m = \{2000, 1000, 500\}$ in Landmark-v2-10K, respectively. For the exemplar-memory size, we used $|\mathcal{M}| = \{5000, 10000, 20000\}$ for Landmark-v2-1K and $|\mathcal{M}| = \{10000, 20000, 30000\}$ for Landmark-v2-10K, respectively. Same as in ImageNet, we used the Ringbuffer approach for constructing the exemplars. For evaluation, we randomly selected 50 and 10 images per each class in Landmark-v2-1K and Landmark-v2-10K that are not in the training set and constructed the test set.

6.2 Implementation detail

The Resnet-18 [13] architecture was used in all experiments, and all the implementation were done with the Pytorch framework[25]. For training the neural network, we always used the stochastic gradient descent (SGD) with initial learning rate 0.1, weight decay 0.0001, and Nesterov momentum 0.9. The batch size used for \mathcal{D}_t , $N_{\mathcal{D}_t}$, was 128, and we used different replay batch size, $N_{\mathcal{M}}$, depending on the number of different incremental states; *i.e.*, $N_{\mathcal{M}} = 16/32/64$ for $T = 20/10/5$, respectively. Thus, the ratio of $N_{\mathcal{D}_t}$

Algorithm 1 SS layer with RP mini-batch

Require: $\{D_t\}_{t=1}^T$: Training dataset
Require: $\mathcal{M} \leftarrow \{\}$: Memory buffer
Require: $\{E\}_{t=1}^T$: The number of epochs per state.
Require: $N_{D_t}, N_{\mathcal{M}}$: Training batch sizes and replay batch sizes
Require: α : Initial learning rate
Require: θ, \mathbf{W}_T : Parameters for feature extractor and linear classifier
Start class incremental learning
 Randomly initialize θ, \mathbf{W}_T
for $t = 1, \dots, T$ **do**
 $\beta = \frac{\alpha}{t+1}$ # learning rate for current state
 for $e = 1, \dots, E_t$ **do**
 # Sample without replacement a mini-batch of size N_{D_t}
 for $B_{D_t} \sim D_t$ **do**
 # Sample with replacement a mini-batch of size $N_{\mathcal{M}}$
 $B_{\mathcal{M}} \sim \mathcal{M}$
 $\mathcal{L}_t = \frac{1}{N_{D_t} + N_{\mathcal{M}}} \sum_{(\mathbf{x}_i, y_i) \in B_{D_t} \cup B_{\mathcal{M}}} \ell((\mathbf{x}_i, y_i), \theta, \mathbf{W}_t)$
 $\theta \leftarrow \theta - \beta \cdot \nabla_{\theta} \mathcal{L}_t$
 $\mathbf{W}_t \leftarrow \mathbf{W}_t - \beta \cdot \nabla_{\mathbf{W}_t} \mathcal{L}_t$
 end for
 end for
 $\mathcal{M} \leftarrow \text{UpdateMemory}(D_t)$
end for

over $N_{\mathcal{M}}$ was $8/4/2$, respectively. The number of epochs for training first incremental state was 100, and the learning rate was divided by 10 at epochs 40 and 80. After training the first state, we reduce the epochs from 100 to 20, and the same learning rate decay was done at epochs 8 and 16. Furthermore, the initial learning rate for each incremental state was set to $\frac{0.1}{t}$. In Section 6.4, we analyze the effect of the number of epochs as well as the replay batch sizes on the performance of our SS-IL. For data pre-processing, the random re-sized cropping and horizontal flipping was adopted to all datasets as data augmentation, and normalization with mean and standard deviation has been performed only for the ImageNet dataset.

We compared our SS-IL with iCaRL[26], vanilla Fine-Tuning (FT) proposed in [4], and IL2M[4]. For iCaRL, as proposed in [17], instead of using binary cross entropy loss for each class output, we used multi-class cross entropy loss for both classification and knowledge distillation loss in iCaRL, which achieves much higher accuracy than the original paper. For FT, as in [4], the number of epochs for training first state was 100. We reduced it to 25 for the incremental states afterwards, and the initial learning rate for all states was set to $\frac{0.1}{t}$. To compare all methods fairly, we reproduced all the baselines and used the same neural network architecture for all methods.

6.3 Results

Table 1 shows the results on Top-1 accuracy, Top-5 accuracy, and the imbalance scores averaged over all the incremental states, for various datasets and evaluation scenarios.

Table 1. The incremental learning results on various datasets and evaluation scenarios. The evaluation metric is average Top-1, Top-5 accuracy, and imbalance score. For average Top-1 and Top-5 accuracy, the higher the number (indicated by \uparrow) the better is the model. For imbalance score, the lower the number (indicated by \downarrow) the better is the model. Best results are in bold.

T	$T = 10$			$ \mathcal{M} = 5k(1K), 10k(10K)$		
Dataset	ImageNet-1K	Landmark-v2-1K	Landmark-v2-10K	ImageNet-1K	Landmark-v2-1K	Landmark-v2-10K
$ \mathcal{M} $	$5k / 10k / 20k$	$5k / 10k / 20k$	$10k / 20k / 30k$	$T = 20 / T = 5$	$T = 20 / T = 5$	$T = 20 / T = 5$
Average Top-1 accuracy(\uparrow)						
iCaRL	41.2 / 45.3 / 47.2	34.8 / 37.8 / 40.1	-	36.2 / 46.8	29.2 / 38.0	-
FT	37.9 / 45.8 / 53.3	43.1 / 50.2 / 57.1	27.4 / 33.5 / 37.8	36.1 / 40.4	37.2 / 48.5	24.2 / 32.5
IL2M	42.2 / 49.0 / 55.4	43.6 / 50.4 / 57.3	28.3 / 34.1 / 38.2	38.3 / 47.4	37.6 / 49.4	24.8 / 33.7
SS-IL	52.6 / 56.3 / 59.3	49.7 / 53.1 / 56.0	36.1 / 40.7 / 43.3	50.2 / 55.3	41.3 / 56.8	37.1 / 36.2
Average Top-5 accuracy(\uparrow)						
iCaRL	65.2 / 70.3 / 72.6	54.5 / 58.8 / 61.5	-	59.5 / 70.6	48.4 / 57.9	-
FT	66.4 / 73.6 / 78.3	63.4 / 69.5 / 74.9	40.9 / 49.1 / 54.0	64.5 / 62.2	57.3 / 67.9	38.9 / 43.2
IL2M	71.1 / 75.9 / 79.8	63.6 / 69.5 / 74.8	41.3 / 49.4 / 54.1	66.0 / 74.7	57.2 / 68.9	38.1 / 45.9
SS-IL	77.5 / 80.4 / 82.9	71.9 / 74.4 / 76.7	52.7 / 57.9 / 60.7	76.3 / 78.9	64.9 / 76.2	54.7 / 49.2
Average imbalance score(\downarrow)						
iCaRL	28.0 / 27.2 / 27.4	31.8 / 31.7 / 31.6	-	27.5 / 28.7	32.7 / 32.9	-
FT	37.7 / 30.7 / 24.3	32.5 / 26.4 / 20.9	43.7 / 38.3 / 34.3	32.6 / 45.6	31.4 / 35.5	40.8 / 47.7
IL2M	32.9 / 27.6 / 22.4	31.9 / 26.0 / 20.8	38.6 / 37.4 / 33.7	30.7 / 31.5	30.9 / 34.3	36.1 / 41.0
SS-IL	20.0 / 19.2 / 18.4	29.8 / 28.9 / 27.4	31.3 / 27.9 / 26.7	21.7 / 25.1	36.0 / 23.5	26.5 / 41.5

The imbalance score was defined to be $\frac{e_t(p,n)+e_t(n,p)}{2}$, in which $e_t(p, n)$ and $e_t(n, p)$ were the ratios of old class test samples misclassified to the new classes and new class test samples misclassified to the old classes, respectively, as also defined in Section 4. Thus, when the imbalance score for CIL method is low, we can say that the classification is making a more balanced decision between the old and new classes. The left half of the table reports the results of fixed $T = 10$ with varying exemplar-memory size $|\mathcal{M}|$, the right half shows the results of fixed $|\mathcal{M}|$ with varying T . Moreover, we could not run iCaRL for Landmark-v2-10K due to time constraint.

From the table, we can make the following observations. Firstly, confirming the result of [4], we observe the vanilla FT always outperforms iCaRL (in terms of accuracy) on all cases except for the ImageNet-1K with $T = 10$, $|\mathcal{M}| = 5k$; *i.e.*, the knowledge distillation, which has been a default approach for CIL since iCaRL, in fact hurts the performance particularly for the large-scale datasets with the exemplar-memory. Secondly, we observe the gain of IL2M, the current state-of-the-art in CIL, over vanilla FT is not as big as the one reported in the original paper [4]. Since the code of the original authors of [4] was not executable, we have re-implemented the method in our experiments. In Section 6.5, we carefully analyze the IL2M and argue why it does not outperform FT significantly. Thirdly, we observe that, for most of the datasets and evaluation scenarios, our SS-IL shows strong performance and achieves significantly higher accuracies than iCaRL, FT and IL2M. Given that IL2M is the current state-of-the-art based on post-processing of FT model scores, this result suggests that our simple modification of FT is very effective. Fourthly, we observe that the imbalance scores of FT tends to be higher

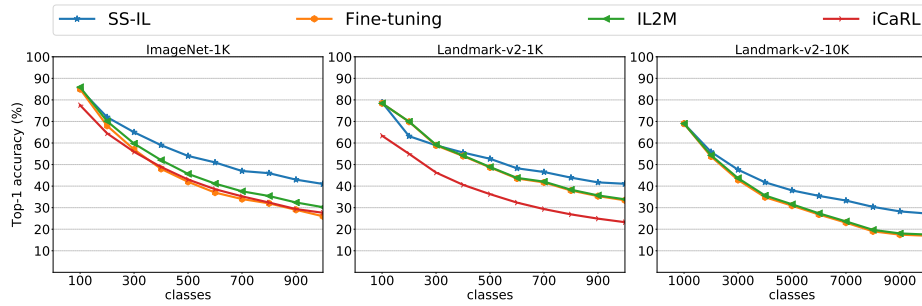


Fig. 4. Incremental learning results on ImageNet-1K, Landmark-1K, and Landmark-10K datasets. The exemplar size is $|\mathcal{M}| = 10k$ in ImageNet-1K and Landmark-1K datasets, and $|\mathcal{M}| = 20k$ in Landmark-v2-10K dataset.

than iCaRL, particularly for the smaller $|\mathcal{M}|$. This makes sense since the data imbalance gets severer as $|\mathcal{M}|$ gets smaller, and the score skewness toward the new class for FT becomes more significant. IL2M does achieve better imbalance score over FT due to the post-processing of the scores, but again, the gain is not very significant. Our SS-IL, on the other hand, achieves significantly better imbalance score compared to the baselines for the most of evaluation scenarios. We also observe the larger $|\mathcal{M}|$, the smaller the imbalance score. We give more detailed analysis on the classification score distribution and imbalance score in Section 6.4.

Figure 4 shows the overall result on each dataset with respect to the incremental state, when $|\mathcal{M}| = 10k$, and the states are denoted as classes. Note SS-IL again mostly dominate the baselines, and the performance gap over the baselines widens as the incremental state increases. Moreover, we observe the performance improvement of IL2M over FT is minor, almost negligible for the Landmark-v2 datasets. This again confirms the ineffectiveness of the bias rectification of IL2M. Furthermore, we observe one of the reasons why iCaRL achieves lower accuracy is due to the weak Nearest Exemplar Mean (NEM) classifier it used, since iCaRL achieves lower accuracy even for the first incremental state.

Figure 5 shows the misclassified error ratios $e_t(p, n)$ and $e_t(n, p)$ more in details for ImageNet-1K dataset with $T = 10$ and $|\mathcal{M}| = 10k$. From the figure, which essentially adds the results of iCaRL and SS-IL to Figure 1, we first observe that $e_t(p, n)$ of FT and IL2M drastically increases as the incremental state increases, while $e_t(n, p)$ is significant small due to the classification score bias. Namely, the most of errors they make are simply due to predicting most of the old classes as the new classes. We note IL2M does improve upon FT after the post-processing, but it still suffers from the heavy bias. Again, we elaborate on this point in Section 6.5. On the other hand, for iCaRL, we observe that $e_t(p, n)$ is significantly lower than those of FT and IL2M, while $e_t(n, p)$ is now much higher than those of FT and IL2M. This suggests that the knowledge distillation of iCaRL does induce to make more predictions

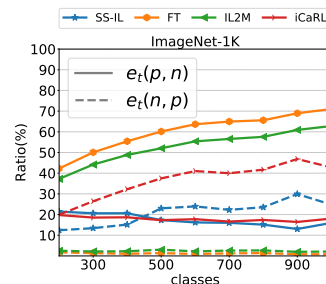


Fig. 5. $e_t(p, n)$ and $e_t(n, p)$ for ImageNet-1K dataset with $T = 10$, $|\mathcal{M}| = 10k$.

toward the old classes, but the low accuracy shows that it hinders the accurate predictions within the old classes. Furthermore, we clearly observe that our SS-IL shows the most balanced error ratios among the methods. That is, we note $e_t(p, n)$ for SS-IL is significantly lower than those of FT and IL2M (similar to that of iCaRL) and $e_t(n, p)$ also stays more or less similar to $e_t(p, n)$ throughout the incremental states. This confirms that our SS layer learned with RP mini-batch makes much more balanced classification decisions, resulting in much fewer confusions between the old and new classes, hence, higher prediction accuracy as shown in Figure 4.

6.4 Analysis and ablation study

In this section, we perform various detailed analyses to show the effectiveness of replay batch sizes, the number of training epochs in SS-IL, and the statistics on prediction scores in both SS-IL and vanilla FT.

Relationship between $N_{\mathcal{M}}$ and T Table 2 shows the results on average Top-1 accuracy and imbalance score with respect to varying replay batch size, $N_{\mathcal{M}}$, and the total number of incremental states, T , for ImageNet-1K. From the table 2, we first observe that when T is large, which corresponds to the case that the number of classes per states, m , is small, the smaller $N_{\mathcal{M}}$ results in the higher average Top-1 accuracy, and when T is small, the larger $N_{\mathcal{M}}$ tends to achieve the higher accuracy. Secondly, we observe that the average accuracy and the average imbalance score are inversely correlated, *i.e.*, as the Top-1 accuracy increases, the

Table 2. Results on ImageNet-1K with varying $N_{\mathcal{M}}$ and T .

$T \setminus N_{\mathcal{M}}$	16 / 32 / 64 / 128
Average Top-1 accuracy	
20	50.2 / 49.0 / 47.7 / 45.1
10	51.5 / 52.6 / 52.9 / 51.9
5	50.7 / 53.2 / 55.3 / 55.2
Average imbalance score	
20	21.7 / 25.3 / 29.1 / 33.2
10	21.7 / 20.0 / 20.3 / 21.5
5	32.3 / 27.6 / 25.1 / 24.3

imbalance score decreases, and vice versa. We believe this is natural as more balanced prediction would result in better accuracy. Finally, when the incremental learning happens frequently enough, *i.e.*, when T is large, we observe $N_{\mathcal{M}} = 128$, which makes the ratio between old and new class samples in the mini-batch to 1 : 1, hurts the accuracy. This suggests that having too many exemplars in the mini-batch would hinder the effective learning of new classes.

The effect of the number of training epochs Figure 6(left) shows the effect of the number of training epochs for each incremental state in SS-IL on ImageNet-1K dataset with $|\mathcal{M}| = 10k, T = 10$. The figure shows the training & test Top-1 accuracy with varying learning epochs in each incremental state. We observe that as the number of epochs gets larger, the training accuracy rises while the test accuracy decreases. This suggests that when the number of epochs is too large, the over-fitting on the training data, $\mathcal{D}_t \cup \mathcal{M}$, happens, and it induces more severe forgetting. Thus, it suggests that a care should be given in preventing the over-fitting while training in CIL algorithms. Thus, using appropriate regularization techniques, *e.g.*, early stopping, should be critically considered while training our SS-IL to prevent catastrophic forgetting.

Analysis on the prediction scores To show the effectiveness of class decision balancing in SS-IL, we analyze the network output prediction scores. Figure 6(center) shows the average prediction scores on test samples for each incremental state t , again for ImageNet-1K with $|\mathcal{M}| = 10k, T = 10$. To see the prediction bias more precisely, we averaged

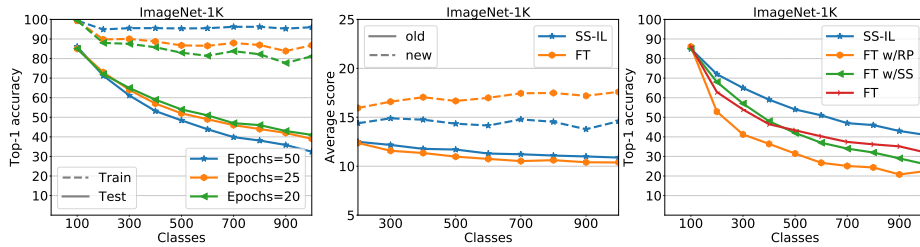


Fig. 6. Experiment results in ImageNet-1K dataset with $|\mathcal{M}| = 10k$. Left: Top-1 accuracy with various training epochs. Center: Average prediction score on test samples. Right: Ablation study on SS-IL.

the prediction scores with respect to old and new classes. In the figure, we observe the average score difference between old and new classes is significant, confirming the score bias toward the new classes mentioned in the earlier sections. Moreover, the gap widens as the incremental state increase. Note this bias results in the heavily skewed error ratios, $e_t(p, n)$ and $e_t(n, p)$, for FT shown in Figure 5. For SS-IL, however, we observe that the average score gap between the old and new classes is much smaller, which suggests that our SS layer and RP mini-batch successfully mitigate the classification scores without the explicit post-processing. Furthermore, the gap does not seem to widen as the incremental state increases, which is desirable for the large-scale data setting.

Ablation study on SS and RP In this section, we validate our approach by ablating each component of SS-IL. Figure 6(right) shows the ablation study results for ImageNet-1K with $|\mathcal{M}| = 10k, T = 10$. In the figure, “FT w/RP” stands for the FT model that selects mini-batches for SGD as in our SS-IL, but does not have the separated softmax layer, “FT w/SS” stands for the FT model that has the separated softmax layer as our SS-IL but randomly selects mini-batches from $\mathcal{D}_t \cup \mathcal{M}$. We observe that “FT w/SS” performs just similarly as FT, and interestingly, “FT w/RP” performs even much worse than the vanilla FT. We clearly observe that SS-IL, which combines both SS and RP mini-batch, largely outperforms the variations of FT, confirming our intuition in devising the method.

To verify the importance of ratio-preserving mini-batch, we apply softmax separation to vanilla FT, which does not use ratio preserving batch. In Figure 6(right), “FT w/SS” achieves lower accuracy than vanilla FT and SS-IL. Surprisingly, after training 400 classes, the performance of “FT w/SS” decreases gradually, and then vanilla FT outperforms “FT w/SS”. Based on above results, using both softmax separation and ratio-preserving mini-batch can remove the prediction bias effectively in training time.

6.5 Discussion on low performance of IL2M [4]

As mentioned in Section 6.3, the performance of IL2M was lower than what was reported in [4]. Since the original result was not reproducible, we give some detailed discussion about our reasoning on the low performance of IL2M.

IL2M rectifies the prediction probability of the old classes with using the statistics of average classification scores, when the prediction results of such classes are the new classes. The rationale is based on the bias in the classification score, so IL2M tries to

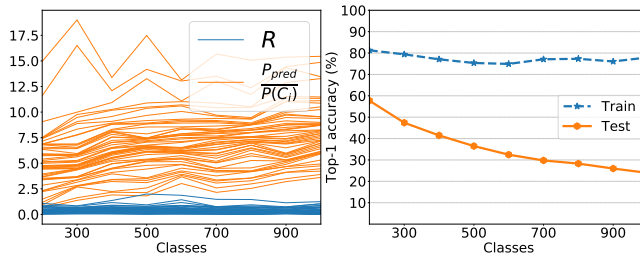


Fig. 7. The analysis on IL2M and vanilla FT.

amplify the the scores for the old classes as an attempt to lower $e_t(p, n)$. For more details on the exact rectification formula, we refer to [4, Eqn.(1)].

Figure 7(left) shows the rectification strength (obtained from the training set), denoted as R , and the ratio of the average of the two probabilities (obtained from the test set) of a vanilla FT model throughout the incremental states; the probability of the predicted class for a test example \mathbf{x} ,

$$P_{\text{pred}} \triangleq \max_y P(y|\mathbf{x}; \boldsymbol{\theta}, \mathbf{W}_t), \quad (4)$$

and the probability of the ground-truth class for \mathbf{x} , denoted as $P(C_i)$ in the figure. The ratio was obtained for the randomly selected 50 classes in the first incremental state with $T = 10$, and Figure 7(right) shows the train & test Top-1 accuracy of vanilla FT for the old classes in each state for ImageNet-1K datasets with $|\mathcal{M}| = 5k$.

Note that the intuition of IL2M is to have R sufficiently large such that when R is multiplied to the probability for the old class that are misclassified to the new class, it can revert the prediction hoping that the rectified probability can be larger than P_{pred} in (4). However, in Figure 7(left), the average probability ratio turns out to be much higher than the rectification strength, R , for the test set, which means that even after rectifying the predicted probability, the predictions may still be unchanged. The main reason for this phenomenon can be found in Figure 7(right), the accuracies for the old classes in each state, which shows that the vanilla FT model is highly over-fitted to the exemplars. Based on this result, due to the over-fitting to exemplars, the statistics $\mu_N(C_i)$ in [4, Eqn.(1)] can become high, hence, R becomes not large enough to correctly rectify the classification probabilities on the test samples.

7 Conclusion

In this paper, we propose a simple class decision balancing methods for CIL, SS-IL, by using separated softmax (SS) layer and ratio-preserving (RP) mini-batches. With extensive experiments and analyses, we show that without applying any post-processing methods, our two simple modifications from vanilla FT achieve higher performance in various large-scale classification datasets, and also show that SS-IL in fact gives much more balanced predictions between the old and new classes than other approaches. Furthermore, we also find that the large number of training epochs can be a serious reason for catastrophic forgetting. By simply reducing the number of training epochs, we show that the Top-1 test accuracy can be increased gradually. Based on these findings,

for further research, we will try to devise a novel and simple algorithms to resolve the catastrophic forgetting problems in class incremental learning.

References

1. Google landmarks dataset v2 (2019), <https://github.com/cvdfoundation/google-landmark>
2. Ahn, H., Cha, S., Lee, D., Moon, T.: Uncertainty-based continual learning with adaptive regularization. In: *Advances in Neural Information Processing Systems*. pp. 4394–4404 (2019)
3. Al-Qizwini, M., Barjasteh, I., Al-Qassab, H., Radha, H.: Deep learning algorithm for autonomous driving using googlenet. In: *2017 IEEE Intelligent Vehicles Symposium (IV)*. pp. 89–96 (June 2017). <https://doi.org/10.1109/IVS.2017.7995703>
4. Belouadah, E., Popescu, A.: I12m: Class incremental learning with dual memory. In: *The IEEE International Conference on Computer Vision (ICCV)* (October 2019)
5. Caruana, R., Lou, Y., Gehrke, J., Koch, P., Sturm, M., Elhadad, N.: Intelligible models for healthcare: Predicting pneumonia risk and hospital 30-day readmission. In: *Proceedings of the 21th ACM SIGKDD International Conference on Knowledge Discovery and Data Mining*. pp. 1721–1730. KDD '15, ACM, New York, NY, USA (2015). <https://doi.org/10.1145/2783258.2788613>, <http://doi.acm.org/10.1145/2783258.2788613>
6. Castro, F.M., Marín-Jiménez, M.J., Guil, N., Schmid, C., Alahari, K.: End-to-end incremental learning. In: *Proceedings of the European Conference on Computer Vision (ECCV)*. pp. 233–248 (2018)
7. Chaudhry, A., Dokania, P.K., Ajanthan, T., Torr, P.H.: Riemannian walk for incremental learning: Understanding forgetting and intransigence. In: *Proceedings of the European Conference on Computer Vision (ECCV)*. pp. 532–547 (2018)
8. Chaudhry, A., Ranzato, M., Rohrbach, M., Elhoseiny, M.: Efficient lifelong learning with a-GEM. In: *International Conference on Learning Representations* (2019), https://openreview.net/forum?id=Hkf2_sC5FX
9. Chaudhry, A., Rohrbach, M., Elhoseiny, M., Ajanthan, T., Dokania, P.K., Torr, P.H., Ranzato, M.: Continual learning with tiny episodic memories. *arXiv preprint arXiv:1902.10486* (2019)
10. Deng, J., Dong, W., Socher, R., Li, L.J., Li, K., Fei-Fei, L.: Imagenet: A large-scale hierarchical image database. In: *2009 IEEE conference on computer vision and pattern recognition* (2009)
11. Goodfellow, I., Pouget-Abadie, J., Mirza, M., Xu, B., Warde-Farley, D., Ozair, S., Courville, A., Bengio, Y.: Generative adversarial nets. In: *Advances in neural information processing systems* (2014)
12. He, K., Zhang, X., Ren, S., Sun, J.: Deep residual learning for image recognition. In: *Computer Vision and Pattern Recognition (CVPR)* (2015)
13. He, K., Zhang, X., Ren, S., Sun, J.: Deep residual learning for image recognition. In: *Proceedings of the IEEE conference on computer vision and pattern recognition*. pp. 770–778 (2016)
14. Hinton, G., LeCun, Y., Bengio, Y.: Deep learning. *Nature* **521**, 436–444 (2015)
15. Hinton, G., Vinyals, O., Dean, J.: Distilling the knowledge in a neural network. *arXiv preprint arXiv:1503.02531* (2015)
16. Hou, S., Pan, X., Loy, C.C., Wang, Z., Lin, D.: Learning a unified classifier incrementally via rebalancing. In: *Proceedings of the IEEE Conference on Computer Vision and Pattern Recognition*. pp. 831–839 (2019)
17. Javed, K., Shafait, F.: Revisiting distillation and incremental classifier learning. In: *Asian Conference on Computer Vision*. pp. 3–17. Springer (2018)
18. Kemker, R., Kanan, C.: Fearnnet: Brain-inspired model for incremental learning. In: *International Conference on Learning Representations (ICLR)* (2018)
19. Kirkpatrick, J., Pascanu, R., Rabinowitz, N., Veness, J., Desjardins, G., Rusu, A.A., Milan, K., Quan, J., Ramalho, T., Grabska-Barwinska, A., Hassabis, D., Clopath, C., Kumaran, D., Hassel, R.: Overcoming catastrophic forgetting in neural networks. *Proceedings of the National*

- Academy of Sciences **114**(13), 3521–3526 (2017). <https://doi.org/10.1073/pnas.1611835114>, <https://www.pnas.org/content/114/13/3521>
20. Lee, K., Lee, K., Shin, J., Lee, H.: Overcoming catastrophic forgetting with unlabeled data in the wild. In: Proceedings of the IEEE International Conference on Computer Vision. pp. 312–321 (2019)
 21. Li, Z., Hoiem, D.: Learning without forgetting. *IEEE Transactions on Pattern Analysis and Machine Intelligence* **40**(12), 2935–2947 (2017)
 22. Lopez-Paz, D., Ranzato, M.A.: Gradient episodic memory for continual learning. In: Advances in Neural Information Processing System (NIPS), pp. 6467–6476 (2017)
 23. Mirza, M., Osindero, S.: Conditional generative adversarial nets. arXiv preprint arXiv:1411.1784 (2014)
 24. Nguyen, C.V., Li, Y., Bui, T.D., Turner, R.E.: Variational continual learning. In: International Conference on Learning Representations (ICLR) (2018), <https://openreview.net/forum?id=BkQqq0gRb>
 25. Paszke, A., Gross, S., Chintala, S., Chanan, G., Yang, E., DeVito, Z., Lin, Z., Desmaison, A., Antiga, L., Lerer, A.: Automatic differentiation in pytorch (2017)
 26. Rebuffi, S.A., Kolesnikov, A., Sperl, G., Lampert, C.H.: icarl: Incremental classifier and representation learning. In: Proceedings of the IEEE Conference on Computer Vision and Pattern Recognition (CVPR). pp. 2001–2010 (2017)
 27. Shin, H., Lee, J.K., Kim, J., Kim, J.: Continual learning with deep generative replay. In: Advances in Neural Information Processing System (NIPS), pp. 2990–2999 (2017)
 28. Wu, Y., Chen, Y., Wang, L., Ye, Y., Liu, Z., Guo, Y., Fu, Y.: Large scale incremental learning. In: Proceedings of the IEEE Conference on Computer Vision and Pattern Recognition. pp. 374–382 (2019)
 29. Xiang, Y., Fu, Y., Ji, P., Huang, H.: Incremental learning using conditional adversarial networks. In: Proceedings of the IEEE International Conference on Computer Vision. pp. 6619–6628 (2019)
 30. Zenke, F., Poole, B., Ganguli, S.: Continual learning through synaptic intelligence. In: International Conference on Machine Learning (ICML). pp. 3987–3995 (2017)